Journal of Membrane Science 366 (2011) 92–96

Contents lists available at ScienceDirect

Journal of Membrane Science

journal homepage: www.elsevier.com/locate/memsci

First-principles electronic-structure calculations on the stability and oxygen conductivity in $Ba_{0.5}Sr_{0.5}Co_{0.8}Fe_{0.2}O_{3-\delta}$

Claudia Wessel, Marck-Willem Lumey*, Richard Dronskowski

Institute of Inorganic Chemistry, RWTH Aachen University, Landoltweg 1, D-52056 Aachen, Germany

ARTICLE INFO

Article history:
Received 24 February 2010
Received in revised form 5 July 2010
Accepted 24 September 2010
Available online 1 October 2010

Keywords:
BSCF
Ionic conductivity
Density–functional theory
CI–NEB method

ABSTRACT

The perovskite-type compound $Ba_{0.5}Sr_{0.5}Co_{0.8}Fe_{0.2}O_{3-\delta}$ has been investigated using quantum–theoretical methods. Density–functional calculations indicate a preference of the oxygen vacancy to be located close to cobalt instead of iron because of the higher affinity of oxygen towards iron. The energy barrier for an oxygen-hopping process was examined using the nudged elastic band (NEB) method. The resulting minimum-energy path is characterized by a correlation between the effective coordination number and the calculated energy: the lower the effective coordination number and the weaker the chemical bonding of the migrating oxygen atoms, the higher the energy. Also, the energy barriers appear to be slightly smaller when the oxygen atom passes an iron atom instead of a cobalt atom. Phonon calculations were carried out to achieve a thermodynamic analysis of B-site substituted BSCF5582 as a function of temperature. Theory suggests that substitution of cobalt by nickel destabilizes the structure whereas Mn-doped BSCF is favored over the unsubstituted compound in a wide temperature range between 0 and 1600 K.

1. Introduction

The development of novel mixed ionic and electronic conducting (MIEC) perovskite-structured materials is nowadays of interest as cathode materials for solid oxide fuel cells [1] and oxygen permeable membranes [2,3]. Therefore, new materials with high oxygen permeation rates are needed. A prototype of such a promising material is given by, for example, $Ba_{0.5}Sr_{0.5}Co_{0.8}Fe_{0.2}O_{3-\delta}$ which has also been dubbed "BSCF5582" in the material-science community. This complex oxide crystallizes in a perovskite-type structure. In order to better understand the atomistic permeation processes, we have used quantum–theoretical methods, in particular to calculate the energy barriers for the oxygen hopping mechanism. In order to numerically evaluate the dependence of this barrier on the crystallographic environment of the moving oxygen atom, various structures with different combinations of the neighboring atoms were analyzed in detail.

2. Theoretical methodology

The total energies and electronic structures of all phases were calculated in the context of density–functional theory. We used the Vienna *ab initio* Simulation Package (VASP) [4–7], together with plane-wave basis sets and ultra-soft pseudopotentials. The contributions of inter-electronic correlation and exchange to the total energies were treated using the generalized-gradient approximation (GGA) [8]. The kinetic energy cut-off of the plane waves was set to 500 eV. For the calculation of saddle points and the minimum energy paths (MEP), the nudged elastic band (NEB) method was applied [9,10], as implemented within VASP. By starting from a well-converged initial and final state, a set of seven in-between images was constructed, and these were connected by artificial spring forces. Within the climbing image (CI)–NEB method [11], the image with the highest energy (climbing image) is identified and moved up the potential surface, thereby achieving a maximum energy. The CI–NEB method, if converged, is known to yield a good approximation for the reaction coordinate around the saddle point.

Thermodynamic quantities at finite temperatures were calculated with the auxiliary program fropho [12], which requires a full structural optimization of the structures in the first step. Then a supercell is created from the optimized structure in order to correctly calculate the Hellmann–Feynman forces by slightly shifting all symmetry-independent atoms away from their equilibrium position. This is needed, first, to determine all force constants and, second, to set up the so-called dynamical matrix. By means of diagonalization, the eigenvalues (phonon frequencies) and the eigenvectors (phonon vibration modi) result which eventually yield the free phonon energy. Together with Bose–Einstein statistics, thermodynamic potentials at finite temperatures are relatively straightforward [13].

* Corresponding author. Tel.: +49 241 80 96089; fax: +49 241 80 92642.
E-mail address: marck.lumey@ac.rwth-aachen.de (M.-W. Lumey).

0376-7388/$ – see front matter © 2010 Elsevier B.V. All rights reserved.
doi:10.1016/j.memsci.2010.09.046

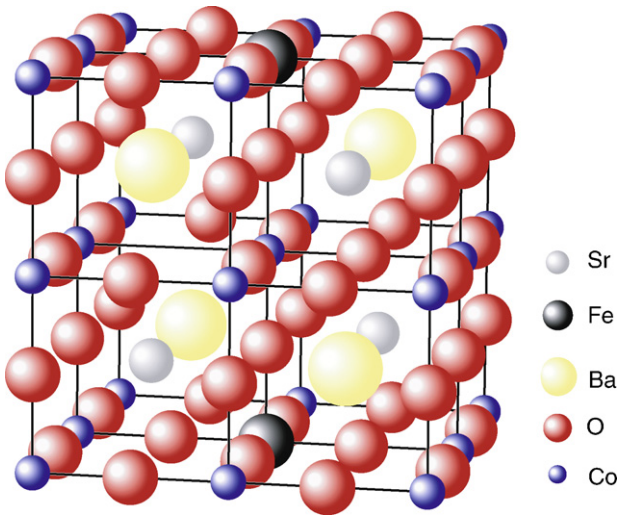

Fig. 1. Example of a supercell of $Ba_{0.5}Sr_{0.5}Co_{0.875}Fe_{0.125}O_{2.875}$ constructed from eight small unit cells and containing 39 atoms; iron atoms are given in black, cobalt in blue, barium in yellow, strontium in grey and oxygen in red. (For interpretation of the references to color in this figure legend, the reader is referred to the web version of the article.)

3. Results and discussion

3.1. Structural properties of $Ba_{0.5}Sr_{0.5}Co_{0.8}Fe_{0.2}O_{3-\delta}$

The crystal structure of $Ba_{0.5}Sr_{0.5}Co_{0.8}Fe_{0.2}O_{3-\delta}$ (BSCF5582) has been described as being a perovskite-type structure [14]. We recall that the regular perovskite structure ABO_3 is relatively simple and contains not more than five atoms in its crystallographic unit cell. In contrast, the construction of a unit cell which corresponds to the composition of BSCF5582 necessitates the use of significantly larger unit cells as a reasonable computational starting point. In the present case, a so-called supercell was generated by doubling the smallest unit cell along each direction ($2 \times 2 \times 2 = 8$). An example of such a supercell, including the eight smaller building blocks, is shown in Fig. 1. We also want to point out that, in order to save precious CPU time which scales with the third power of the system's size, the exact composition within the cationic sublattice of BSCF5582 was slightly simplified.

To allow for oxygen conductivity, BSCF5582 requires vacancies within the oxygen sublattice. In a first approximation we removed one oxygen atom in the computational supercell, and this leads to a composition of $Ba_{0.5}Sr_{0.5}Co_{0.875}Fe_{0.125}O_{2.875}\square_{0.125}$. Since an oxygen atom is octahedrally surrounded by $2 + 4 = 6$ cations and BSCF5582 contains four different cations, there is a multitude of possible positions for this vacancy. At the beginning, one needs to find out which atomic site is preferred by an oxygen vacancy. A set of four different arrangements was therefore created, two times with a vacancy between an iron and a cobalt atom and two times between two adjacent cobalt atoms. The latter two arrangements differ with respect to the strontium and barium arrangements within the second coordination shell. In order to compare these configurations, their entire crystal structures were computationally optimized on the basis of the corresponding total energy. Since the high symmetry of the starting perovskite structure is broken by the removal of one oxygen atom, significant structural deformations are to be expected. The results of these calculations are shown in Table 1.

It is quite obvious that the oxygen vacancy prefers the position between two cobalt atoms, and the oxygen atoms also tends to stay in the proximity of the iron atom. This atomistic observation is nicely related to the fact that, macroscopically, iron has a considerably larger affinity towards oxygen than cobalt, as given by the free energies of combustion: $\Delta G^{1873\,K}(FeO) = -147$ kJ/mol and $\Delta G^{1873\,K}(CoO) = -101$ kJ/mol [15]. Moreover, it is remarkable that only in one case of "Fe–□–Co" structural set-up, one finds a major deformations of the lattice and also the atomic sites. In this particular case, the cubic perovskite supercell ($a = 7.82$ Å) changes into an orthorhombic cell with lattice parameters of $a = 7.29$ Å, $b = 9.45$ Å and $c = 8.07$ Å. Even more astonishing is the fact that the pseudo-octahedral environment of the iron atom ($5 \times O$ and $1 \times \square$) re-arranges into a tetrahedron-like surrounding with four nearest-neighbor oxygen atoms. In contrast to this, the two cases where the oxygen defect is located between two cobalt atoms do not suffer from such larger distortions, and there are only minor changes with respect to the supercell; thus, the perovskite-like structure seems to stay intact.

Table 1
Calculated total energies for $Ba_{0.5}Sr_{0.5}Co_{0.875}Fe_{0.125}O_{2.875}$ with one oxygen vacancy, located at three different positions.

Configuration	Energy (eV/cell)
Co–□–Co	−254.81
Co–□–Co[a]	−254.61
Fe–□–Co	−254.53
Fe–□–Co[a]	−253.45

[a] Different strontium and barium arrangements

3.2. Transport properties of $Ba_{0.5}Sr_{0.5}Co_{0.8}Fe_{0.2}O_{3-\delta}$

After having analyzed the preferred location of the oxygen vacancy, the energy barrier for an oxygen hopping process was calculated. Here, the oxygen atom jumps from its original position into the created vacancy. The standard calculational procedure proceeds by first structurally optimizing the starting and the final structures for such a hopping process. It should be noted that in our case only one oxygen atom jumps into a nearby vacancy at a given time. In the upper part of Fig. 2 the octahedral environment of the oxygen atom at the beginning and at the final point of the atomic migration has been depicted. In the here implemented migration path the oxygen atom moves through a trigonal plane which is shared by two adjacent octahedra. In order to calculate the transport properties of BSCF5582, a set of seven images between the starting and final point was generated.

A more detailed view of this hopping process, is also shown in the bottom of Fig. 2. Only the oxygen atom and the three atoms forming the trigonal plane are allowed to move while the rest of the lattice is structurally kept fixed; otherwise, the computational demands would be extraordinarily large. The energy of each single image is correctly calculated without any human intervention but the images are coupled with each other through so-called artificial spring forces which simply prevent that an oxygen atom moving through a high-energy structural configuration falls back into either the starting or the final configuration.

Let us focus on the results of two calculations where the saddle-point configurations are characterized by the presence of three metal atoms forming the triangles, dubbed as Δ_{SrBaCo} and Δ_{SrBaFe}. The calculated energy profiles corresponding to the oxygen atom moving through these saddle-point configurations are shown in Fig. 3. The shape of the curve can be explained by an evaluation of the effective coordination number of the O atom according to the recipe of Brunner and Schwarzenbach [16] as this atom passes through the triangle. The calculated effective coordination numbers (ECoN) for the various images are listed in Table 2.

By comparing the ECoN and the energy profile in Fig. 3, it becomes obvious that the maximum energy is found for the image in which the O atom experiences the lowest effective coordination number, namely image no. 5.